ADVANCED MATERIALS

Supporting Information

for *Adv. Mater.*, DOI 10.1002/adma.202303357

Flagella of Tumor-Targeting Bacteria Trigger Local Hemorrhage to Reprogram Tumor-Associated Macrophages for Improved Antitumor Therapy

*Haiheng Xu, Shuqin Xiong, Yiyun Chen, Qingsong Ye, Nan Guan, Yiqiao Hu and Jinhui Wu**

Supporting Information

Flagella of Tumor-targeting Bacteria Trigger Local Hemorrhage to Reprogram Tumor-associated Macrophages for Improved Antitumor Therapy

*Haiheng Xu, Shuqin Xiong, Yiyun Chen, Qingsong Ye, Nan Guan, Yiqiao Hu, and Jinhui Wu**

Supplementary methods

Stability evaluation of flhDC VNP: flhDC VNP were cultured in LB medium with arabinose (absin, 0.02 M). flhDC VNP were transferred to new LB medium every 12 h at a ratio of 1:100, and continuously passed for 8 generations. The bacteria of each generation were resuspended in sterile water after centrifugation (3000 rpm, 5 min), and optical density (OD_{600}) was adjusted to 10. The overexpressed protein was detected using Coomassie Brilliant Blue staining (Beyotime).

Scanning electron microscopy (SEM) of bacteria: The bacteria (flhDC VNP, ΔflhD VNP, and VNP) were cultured overnight, diluted 1:100 into LB medium, and grew to OD_{600} ~0.8. Bacteria were collected and washed 3 times with sterile water. Bacterial suspension (10 μL) was dropped on the silicon wafer and dried by infrared. The samples were sputter coated with gold prior to imaging. High-resolution SEM images were obtained using GeminiSEM 500 (Zeiss) at a beam voltage of 5 kV, and a working distance of < 5.6 mm. Electron microscope pseudocolor was performed using photoshop.

Motility evaluation of bacteria: First, the motility of bacteria (flhDC VNP, ΔflhD VNP, and VNP) were measured in a 0.2% agar-enclosed transwell system. Briefly, the 8 μm micropores of the transwell were first enclosed using 0.2% agar. Bacteria (flhDC VNP, ΔflhD VNP, and VNP, approximately 5×10^8 CFU mL^{-1};100 μL) and medium (500 μL) per well were then respectively added into the apical and basolateral chamber. After 1 and 2 h, medium (50 μL) in basolateral chamber was plated on LB plates. After 12 h of incubation, bacterial colonies on LB plates were counted.

Next, the motility of bacteria (flhDC VNP, ΔflhD VNP, and VNP) was measured in 3D tumor cell sphere. Briefly, CT26 tumor cells (approximately 4×10^3) were seeded in a round-

bottom 96-well plate (Corning). After 2 days, SYTO9 (Invitrogen)-stained bacteria (flhDC VNP, ΔflhD VNP, and VNP, approximately 1×10^9 CFU mL^{-1};100 μL) were added to 3D cell spheroids. After 5 h, the penetration of bacteria inside the 3D cell spheroid was detected using confocal laser scanning microscope (Olympus, FV3000). Fluorescence quantification was performed by Image J.

Bacterial colonization in vivo: Tumor-bearing mice were treated with flhDC VNP, ΔflhD VNP, and VNP (approximately 2×10^6 CFU per mouse) by intravenous injection. At desired time points, the major organs, including heart, liver, spleen, lung, kidney, and tumor, were extracted, weighed, and homogenized at 4 °C in sterile PBS. The tissue and blood samples were diluted and plated on LB plates. After 12 h of incubation, bacterial colonies were counted. The bacterial titer (CFU per gram of tissue) was calculated with colony counts and tissue weights.

Evaluation of inflammatory cytokine secretion in serum induced by bacteria: Tumor-bearing mice were treated with flhDC VNP, ΔflhD VNP, and VNP (approximately 2×10^6 CFU per mouse). The blood samples were collected at desired time points, rested for 1 h, and then centrifuged (3000 rpm, 15 min, 4 °C). The supernatant was collected for TNFα ELISA assays (DAKEWE).

The effect of TNFα blocking on tumor hemorrhage: CT26 tumor-bearing mice were treated with saline, flhDC VNP, and flhDC VNP + anti-TNFα (flhDC VNP, approximately 2×10^6 CFU per mouse; anti-TNFα, BioLegend, 10 mg kg^{-1}) for 12 h. To neutralize TNFα, mice were pre-treated with anti-mouse TNFα by intraperitoneal injections 24 h before the injection of flhDC VNP. To test the hemoglobin content in tumors, the collected tumors were weighted and homogenized in 1 mL ice-cold sterile PBS. ACK lysis buffer (Bio-Channel) was then added for 10 min. Afterwards, the samples were centrifuged (13,000 rpm, 10 min) and optical density at 540 nm of the supernatants was recorded.

Evaluation of hemorrhage in different tumors induced by flhDC VNP: Breast cancer 4T1-bearing BALB/c mice and melanoma B16OVA-bearing C57BL/6 mice were treated with flhDC VNP (approximately 1×10^7 CFU per mouse) for 12 h. The collected tumor tissues were weighted and homogenized in 1 mL ice-cold sterile PBS. ACK lysis buffer (Bio-

Channel) was then added for 10 min. Afterward, the samples were centrifuged (13,000 rpm, 10 min), and optical density at 540 nm of the supernatants was recorded.

Evaluation of Arts binding to heme or hemoglobin: Hemin (Energy Chemical, 4×10^{-3} M) in DMSO (10 μL), Arts (Macklin, 0.02 M) in DMSO (10 μL), and dithionite (MERYER, 2×10^{-3} M) in PBS (980 μL) were mixed and the UV–vis spectra were measured. To generate heme through reduction of hemin, dithionite was added.

Hemoglobin (MACKLIN, 4.64×10^{-5} M) in PBS (50 μL), Arts (MACKLIN, 4.65×10^{-3} M) in saline (10 μL) and 980 μL PBS were mixed and the UV–vis spectra were measured.

Evaluation of peroxidase activity: Peroxidase activity was measured in PBS (pH 7.0) using H_2O_2 (0.025 M) and ABTS (XiYashiji, 2.8×10^{-3} M) as chromogenic reducing substrate. Heme (7×10^{-5} M) and Arts (MACKLIN, 2.8×10^{-3} M) were preincubated in buffer containing ABTS for varying times, and the reaction initiated by addition of H_2O_2. Formation of $ABTS^+$, the oxidation product, was monitored at 660 nm. Peroxidase activity was calculated from the slope of the initial linear portion of the reaction.

RAW264.7 cells (approximately 2×10^5) were seeded in 24-well plates with cell climbing slices and treated with PBS, RBC, Arts, and RBC + Arts (RBC, approximately 3×10^7 cells mL^{-1}; Arts, 1×10^{-5} M). After 12 h, the medium was removed and 300 μL TMB (MACKLIN) solution was added for 30 min. Finally, the cell climbing slices were taken out and measured using Pannoramic MIDI (3D histech).

To measurement of intratumoral peroxidase activity in vivo, tumor-bearing mice were treated with saline, ΔflhD VNP, VNP, flhDC VNP, Arts, ΔflhD VNP + Arts, VNP + Arts, and flhDC VNP + Arts (bacteria, approximately 2×10^6 CFU per mouse; Arts, 15 mg kg^{-1}). After 12 h, the tumor tissues were collected and sectioned at 8 μm. 300 μL TMB (MACKLIN) solution was added to tumor tissues for 30 min. Then, the tumor tissues were measured using Pannoramic MIDI (3D histech).

Erythrophagocytosis of macrophages: RAW264.7 cells (approximately 2×10^5) were seeded in 24-well plates with cell climbing slices. DIO-stained RBC (approximately 3×10^7 cells mL^{-1}) were added to the RAW264.7 cells. After 6 h, the cell climbing slices were measured by confocal laser scanning microscope (Olympus, FV3000). The cells were resuspended, and the phagocytosis of RBC was measured by flow cytometry (BD FACS Callibur). The data from flow cytometry were analyzed using FlowJo software.

Detection of intracellular heme content after erythrophagocytosis: RAW264.7 cells (approximately 2×10^5) were seeded in 24-well plates and treated with RBC (approximately 3×10^7 cells mL^{-1}) for 6 and 10 h. The cells were collected, and ACK lysis buffer (Bio-Channel) was added for 5 min. The oxalic acid (Shanghai yuanye) was added and then heating at 95 °C for 30 min. Fluorescence (Ex/Em = 400/662 nm) of the resultant protoporphyrin was measured by microplate reader (Molecular Devices M3). The endogenous protoporphyrin content measured in parallel unheated samples in oxalic acid was subtracted.

Evaluation of inflammatory cytokine secretion induced by RBC and Arts: RAW264.7 cells (approximately 2×10^5) were seeded in 24-well plates and treated with PBS, RBC, Arts, and RBC + Arts (RBC, approximately 3×10^7 cells mL^{-1}; Arts, 1×10^{-5} M) for 24 h. The cytokines in supernatant were measured using TNFα and IL-6 ELISA kit (DAKEWE).

The effects of RBC on the pro-inflammatory polarization of macrophages: RAW264.7 cells (approximately 2×10^5) were seeded in 24-well plates and treated with RBC (approximately 3×10^7 cells mL^{-1}) for 3, 6, and 9 h, respectively. Then, the cells were stained with FITC anti-mouse CD86 and APC anti-mouse CD80 (BioLegend) and detected by flow cytometry (Beckman Coulter Cytoflex S). In vivo, tumor-bearing mice were treated with RBC (approximately 5×10^9 cells per mouse) for 12, 24, 48, and 72 h by intratumoral injection. Then, the tumor tissues were collected, stained with PE anti-mouse F4/80, FITC anti-mouse CD86, and APC anti-mouse CD80 (BioLegend), and detected by flow cytometry (Beckman Coulter Cytoflex S). The data from flow cytometry were analyzed using FlowJo software.

Cytotoxicity study: RAW264.7 cells (approximately 2×10^5) were seeded in 24-well plates and treated with a series of dilutions of Arts and Arts + RBC (RBC, approximately 3×10^7 cells mL^{-1}) for 12 h. RAW264.7 cells viability was measured by the staining of 7-AAD viability staining solution (BioLegend) through flow cytometry (BD FACS Callibur). The data from flow cytometry were analyzed using FlowJo software.

The detection of respiration of macrophage mitochondria by Seahorse assay: The assay was performed with the XF Cell Mito Stress Test Kit (Seahorse Bioscience). RAW264.7 cells (approximately 1×10^4) were seeded in 96-well cell plate with 500 μL growth medium for 24 h and treated with RBC and RBC + Arts (RBC, approximately 3×10^7 cells mL^{-1}; Arts, 1 ×

10^{-5} M) for 12 h. Meanwhile, the sensor cartridge was hydrated overnight. The cells were washed twice according to the manufacturer's instructions before the assay. The oxygen consumption rate (OCR) was measured by Seahorse XF96 extracellular flux analyzer (Seahorse Bioscience) to assess the mitochondrial function.

Transcriptome analysis: For transcriptome analysis of tumor, tumors were collected, cut into 0.5 cm^3 and washed with RNase-Free PBS after treatment about 3 days in the xenograft colon tumor model. Then, the tumor fragments were submerged in RNAlater (Ambion). For transcriptome analysis of RAW264.7 cells, RAW264.7 cells (approximately 1×10^6) were seeded in 6-well plates and treated with PBS, RBC, Arts, and RBC + Arts (RBC, approximately 3×10^7 cells mL^{-1}; Arts, 1×10^{-5} M) for 12 h. The total RNA of the samples was extracted using TRIzol (ThermoFisher, 15596018) and purified following the protocol provided by the manufacturer. The concentration and purity of the total RNA were analyzed by NanoDrop ND-1000 (NanoDrop), and the integrity was detected by Bioanalyzer 2100 (Agilent). The downstream experiments were performed when the concentration of total RNA > 50 ng μL^{-1}, RIN value > 7.0 and the total RNA >1 μg. The mRNA containing poly (A) tail was captured specifically by Dynabeads Oligo (dT) (Thermo Fisher, cat. 25-61005) through two-step purification. The captured mRNA was fragmented at 94 °C for 5-7 min using NEBNextR Magnesium RNA Fragmentation Module Kit (NEB, cat. E6150S). The fragmented RNA was reverse transcripted into cDNA using the Invitrogen SuperScriptTM°II Reverse Transcriptase Kit (Invitrogen, cat. 1896649). Then the double-strand synthesis was performed by E. coli DNA polymerase I (NEB, cat. m0209) and RNase H (NEB, cat. m0297). During this process, the DNA-RNA hybrid was transformed to double-strand DNA, and the dUTP (Thermo Fisher, cat. R0133) was added into the double-strand DNA to form the blunt ends. Both ends of the DNA were modified by an adenine for linking to the end containing thymine, then the size of the fragment was filtered and the fragment was purified by the beads. The fragment was digested by Uracil-DNA Glycosylase (NEB, cat. m0280). The DNA fragment was amplified by PCR to form the chain-specific library, fragment size of which is 300 bp ± 50 bp. The PCR was performed by using 95 °C for 3 min for the initial denaturation. Eight cycles in total were then performed by using 98 °C denaturation for 15 s, 60 °C annealing for 15 s and 72 °C extension for 30 s. The total extension was performed at 72 °C for 5 min. At last, the paired-end sequencing was performed by illumina NovaseqTM 6000 (LC Bio Technology CO., Ltd. Hangzhou, China) with the mode PE150.

Secretion of chemokines of macrophages induced by RBC and Arts: RAW264.7 cells (approximately 2×10^5) were seeded in 24-well plates and treated with PBS, RBC, Arts, and RBC + Arts (RBC, approximately 3×10^7 cells mL^{-1}; Arts, 1×10^{-5} M) for 3 h. The expression of CXCL11 was detected by WB.

The effects of flagella on the pro-inflammatory polarization of macrophages: RAW264.7 cells (approximately 2×10^5) were seeded in 24-well plates and treated with ΔflhD VNP and flhDC VNP (approximately 6×10^6 CFU mL^{-1}) for 3 h. Then, the TNFα in supernatant was measured using TNFα ELISA kit (DAKEWE).

TNFα production in tumor induced by flhDC VNP: CT26 tumor-bearing mice were treated with flhDC VNP (approximately 2×10^6 CFU per mouse) for 48 h. The collected tumor tissues were weighted and homogenized in 1 mL ice-cold sterile saline. The samples were centrifuged (3000 rpm, 10 min, 4 °C). Then, the TNFα in supernatant was measured using TNFα ELISA kit (DAKEWE).

The detection of expression of HMOX-1: RAW264.7 cells (approximately 2×10^5) were seeded in 24-well plates and treated with PBS, RBC, Arts, and RBC + Arts (RBC, 3×10^7 cells mL^{-1}; Arts, 1×10^{-5} M) for 3, 9, and 12 h, respectively. Total RNA of RAW264.7 cells was extracted using TranszolUp Reagent (TransGen Biotech). For detection of HMOX-1 in vivo, tumor-bearing mice were treated with saline, flhDC VNP, and flhDC VNP + Arts (flhDC VNP, approximately 2×10^6 CFU per mouse; Arts, 15mg kg^{-1}). After 24 and 72 h, tumor tissues were collected and weighed. Tumor tissues (50-100 mg) were frozen in liquid nitrogen. Then, tumors were ground into powder and dissolved in 1mL Trizol (TransGen Biotech). Total RNA of tumors was extracted using TranszolUp Reagent (TransGen Biotech). The complementary DNA (cDNA) of RAW264.7 cells and tumor tissues were synthesized and purified by TransScript All-in-One First-Strand cDNA Synthesis kit (TransGen Biotech). Quantitative Reverse Transcription-PCR (qRT-PCR) was then performed using PerfectStart Green qPCR SuperMix (TransGen Biotech) in the QuantStudio 5 Real-Time PCR System (Applied Biosystems) using the primers of HMOX-1 (primer 1: CAGTCCCAAACCTCGCGGT sequence; primer 2: GCTGTGCAGGTGTTGAGCC sequence). Data were analyzed using the $2^{(-\Delta\Delta Ct)}$ method and normalized to β-actin expression.

The detection of expression of MHC- Ⅱ *of macrophages:* RAW264.7 cells (approximately 2×10^5) were seeded in 24-well plates and treated with PBS, RBC, Arts, and RBC + Arts (RBC, approximately 3×10^7 cells mL^{-1}; Arts, 1×10^{-5} M) for 3, 9, and 12 h, respectively. Then, the cells were stained with APC anti-mouse I-A/I-E (BioLegend) and detected by flow cytometry (Beckman Coulter Cytoflex S). Tumor-bearing mice were treated with saline, flhDC VNP, and flhDC VNP + Arts (flhDC VNP, approximately 2×10^6 CFU per mouse; Arts, 15mg kg^{-1}). After 24 and 72 h, tumor tissues were collected, stained with PE anti-mouse F4/80 and APC anti-mouse I-A/I-E (BioLegend), and detected by flow cytometry (Beckman Coulter Cytoflex S). Data from flow cytometry were analyzed using FlowJo software.

Safety evaluation: On the 10^{th} day of the antitumor efficacy assay in the xenograft colon tumor model, the major organs of mice were collected including heart, liver, spleen, lung, and kidney. Safety evaluation was measured using H&E staining. To study the safety of multiple administrations of flhDC VNP, healthy BALB/c mice were injected with flhDC VNP (approximately 2×10^6 CFU per mouse) intravenously three times on days 1, 8 and 15. Mouse weights were measured every two days for 21 d.

Supplementary figures

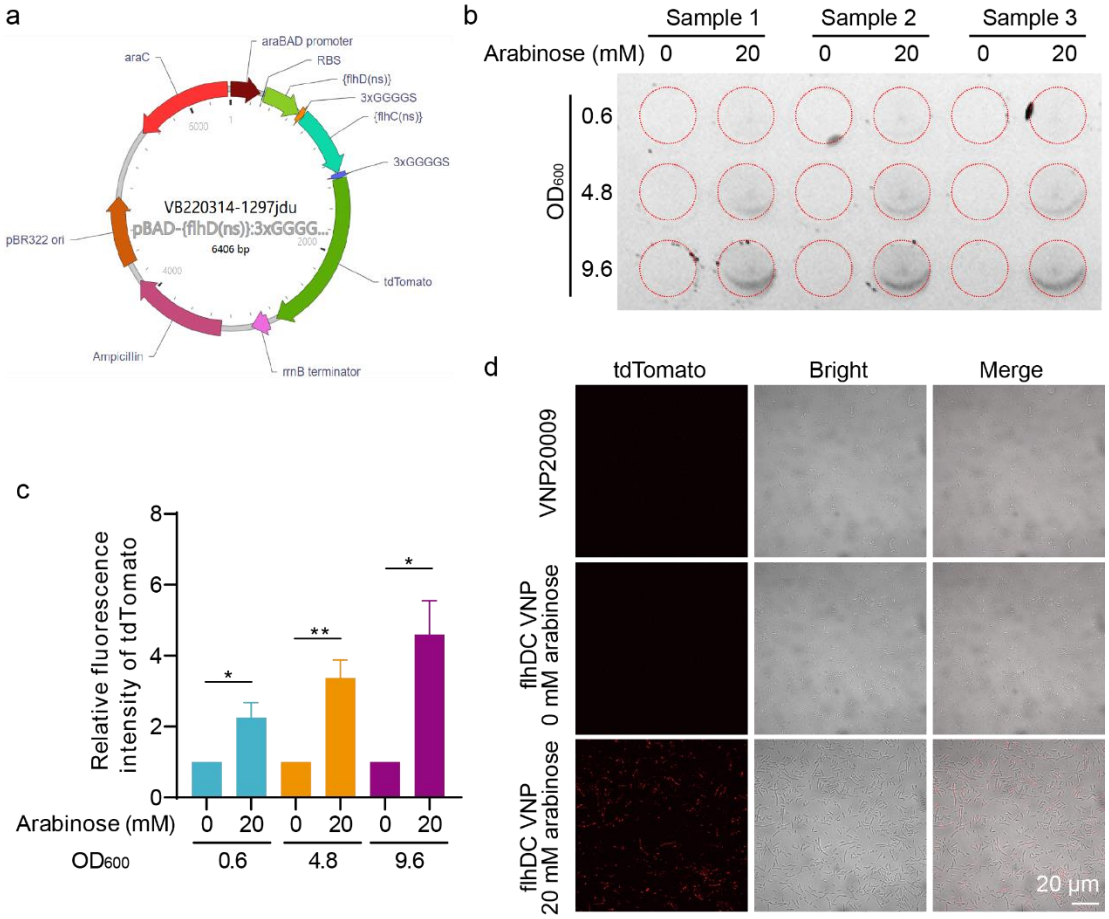


Figure S1. Fluorescence characterization of the flhDC VNP. a) pBAD-flhDC plasmid map. b) Fluorescence images of flhDC VNP (grey) with or without arabinose induction. Red circles represented fluorescent wells. c) Fluorescence quantification of flhDC VNP with or without arabinose induction in (b) (n = 3). d) Representative fluorescence images of VNP and flhDC VNP with or without arabinose induction. Scale bar, 20 μm. In (c), data are mean ± s.e.m. Statistical analysis was performed using two-sided unpaired Student's *t*-tests (c). **P* < 0.05, ***P* < 0.01.

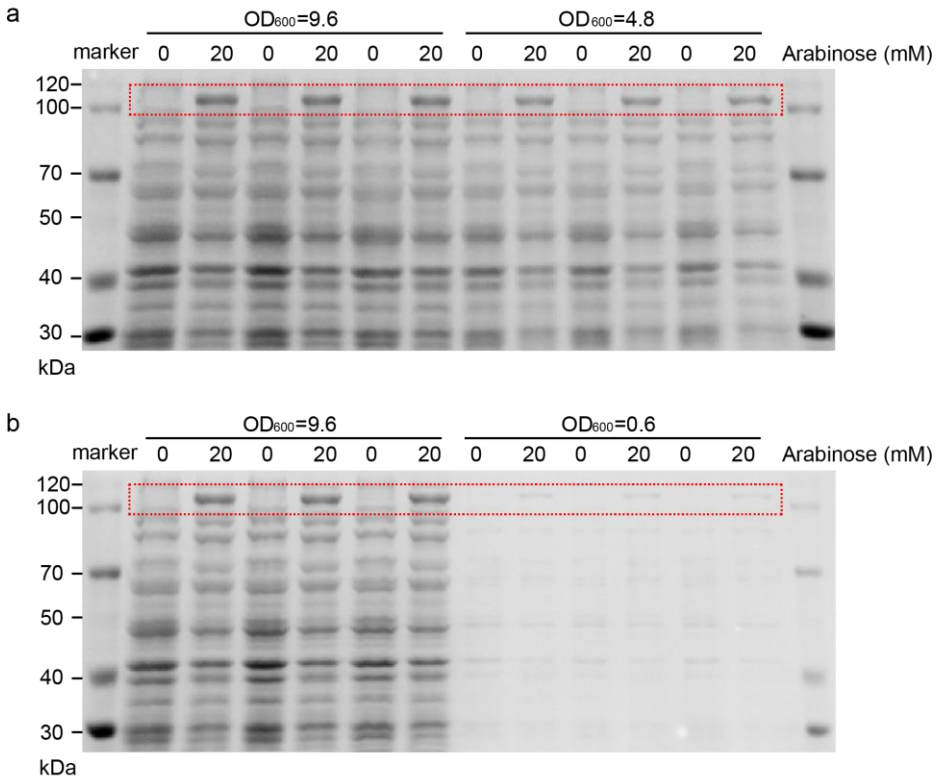


Figure S2. Characterization of target protein expression. a,b) SDS-PAGE images of flhDC VNP with or without arabinose induction. Red box represents the position of overexpressed target protein.

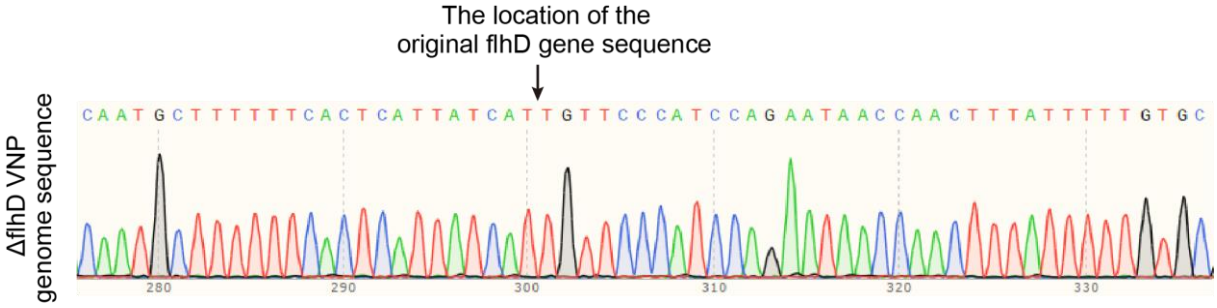


Figure S3. Genome sequence of ΔflhD VNP.

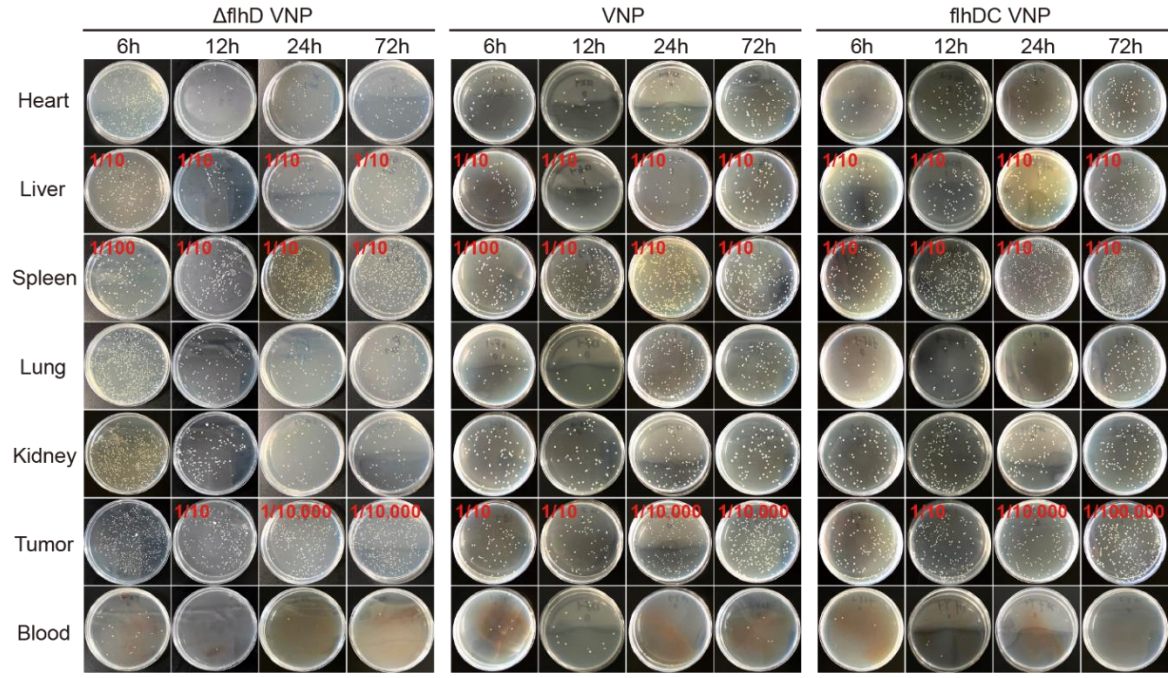


Figure S4. Representative photographs of LB plates of bacteria colonization in various organs. Representative photographs of LB plates of bacterial colonization in various organs harvested from CT26-bearing mice at different time points after injection of bacteria (flhDC VNP, ΔflhD VNP, and VNP). Red numbers represent the dilution factors.

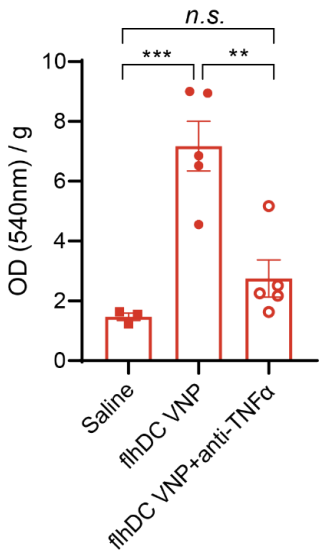


Figure S5. The effect of TNFα blocking on tumor hemorrhage. Intratumoral Hb content of CT26 bearing mice treated with saline, flhDC VNP, and flhDC VNP + anti-TNFα for 12 h (saline, n = 3; flhDC VNP, flhDC VNP + anti-TNFα, n = 5). Data are mean ± s.e.m. Statistical analysis was performed using one-way ANOVA with Dunnett's test. $^{**}P < 0.01$, $^{***}P < 0.001$, *n.s.* means no significance.

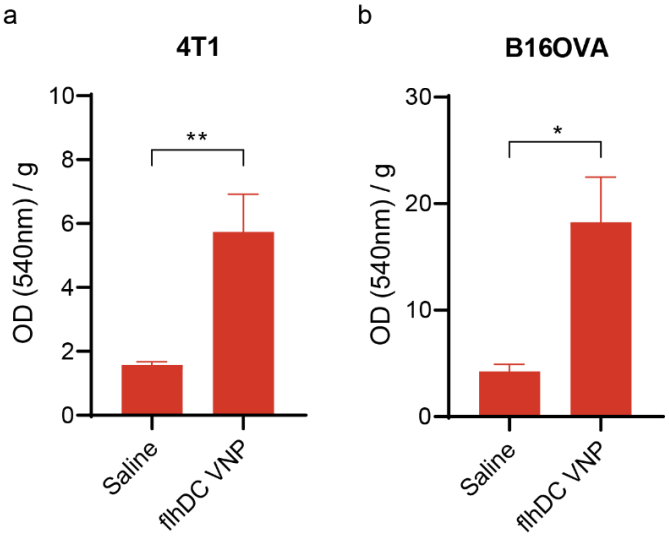


Figure S6. Intratumoral Hb content in breast cancer 4T1 (a, n = 5) and melanoma B16OVA (b, n = 3) after treated with flhDC VNP for 12 h. Data are mean ± s.e.m. Statistical analysis was performed using two-sided unpaired Student's t-tests. *$P < 0.05$, **$P < 0.01$.

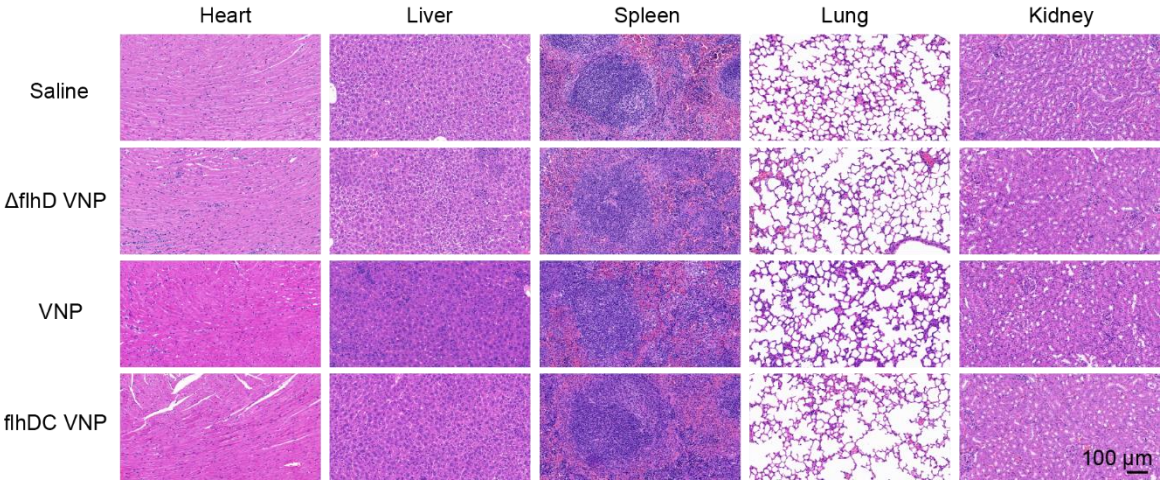


Figure S7. H&E from major organs after systemic administration of bacteria. The major organs of mice were collected including heart, liver, spleen, lung, and kidney on the 10th day of the antitumor efficacy assay in the xenograft colon tumor model. Scale bar, 100 μm.

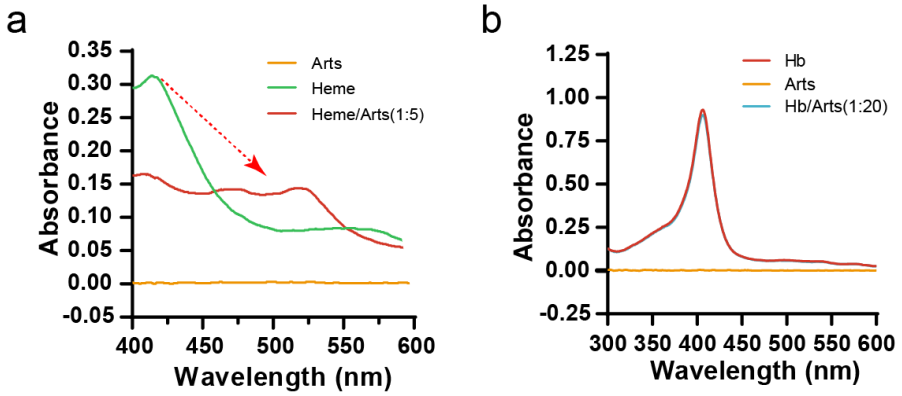


Figure S8. a) UV-vis spectra of the reaction of Arts and heme. Red arrow represents the shifts of the characteristic absorption peak. b) UV-vis spectra of the reaction of Arts and Hb.

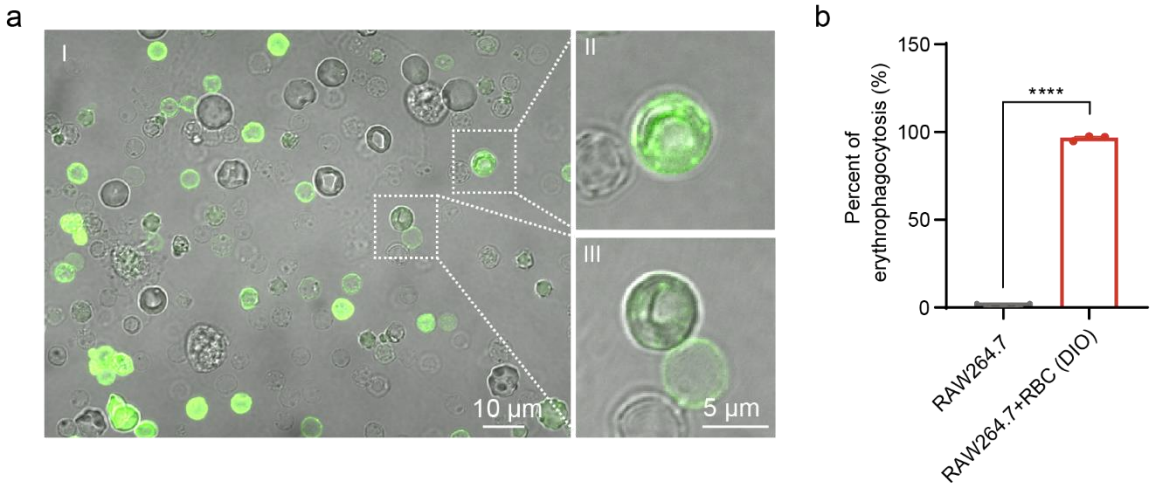


Figure S9. Characterization of erythrophagocytosis of macrophages. a) Representative fluorescent images of erythrophagocytosis of RAW264.7 cells for 6 h. RBC were labeled with DIO (green). Scale bars, 10 μm (image I) and 5 μm (image II and III). b) Flow cytometric analysis of percent of erythrophagocytosis of RAW264.7 cells (n = 3). In (b), data are mean ± s.e.m. Statistical analysis was performed using two-sided unpaired Student's *t*-tests (b). ****$P < 0.0001$.

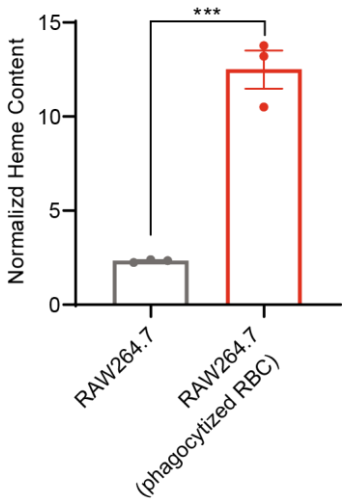


Figure S10. Intracellular heme content of RAW264.7 cells with or without phagocytosing RBC. Data are mean ± s.e.m. Statistical analysis was performed using two-sided unpaired Student's t-tests. ***$P < 0.001$.

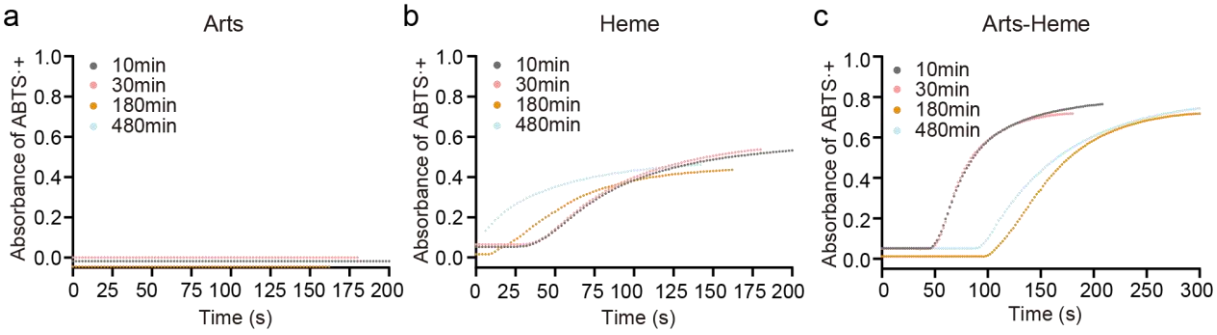


Figure S11. Characterization of peroxidase activity of Arts-Heme complex. a-c) Heme was preincubated with Arts for the times indicated (10, 30, 180, and 480 min), then H_2O_2 was added, and the peroxide activity was measured by the initial rate of ABTS oxidation.

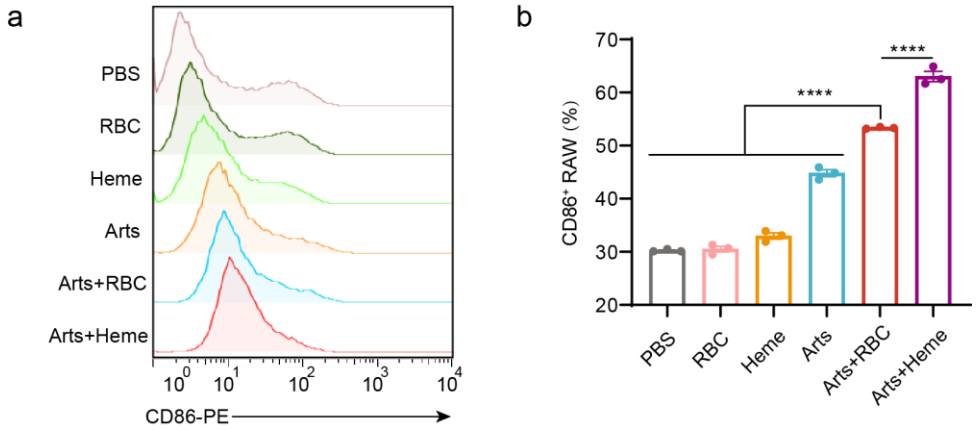


Figure S12. Pro-inflammatory characterization of Arts and Heme. a,b) Representative flow cytometry plots (a) and flow cytometric analysis (b) of RAW264.7 cells with different treatments for 12 h (n = 3). In (b), data are mean ± s.e.m. Statistical analysis was performed using one-way ANOVA with Dunnett's test (b). ****$P < 0.0001$.

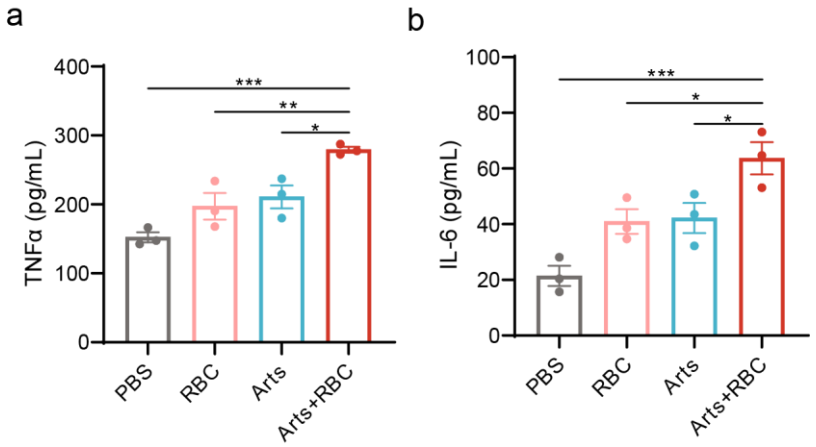


Figure S13. Secretion of inflammatory factors by macrophages. a,b) The concentration of inflammatory factors TNFα (a) and IL-6 (b) released from RAW264.7 cells after different treatments for 24 h (n = 3). In (a, b), data are mean ± s.e.m. Statistical analysis was performed using one-way ANOVA with Dunnett's test (a, b). *$P < 0.05$, **$P < 0.01$, ***$P < 0.001$.

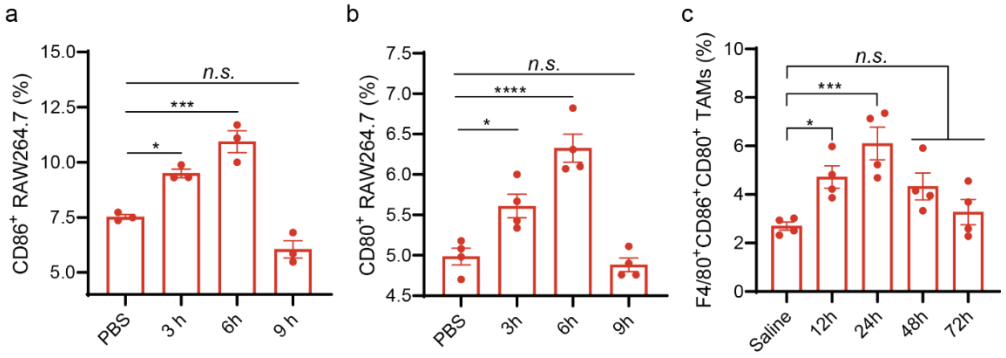


Figure S14. The effects of RBC on the pro-inflammatory polarization of macrophages. a,b) Flow cytometric analysis of $CD86^+$ RAW264.7 cells (a, n = 3) and $CD80^+$ RAW264.7 cells (b, n = 4) after treatment with RBC for different times in vitro. c) Flow cytometric analysis of $F4/80^+CD86^+$ $CD80^+$ TAMs after intratumoral injection of RBC at different times (n = 4). In (a-c), data are mean ± s.e.m. Statistical analysis was performed using one-way ANOVA with Dunnett's test (a-c). $*P < 0.05$, $***P < 0.001$, $****P < 0.0001$, *n.s.* means no significance.

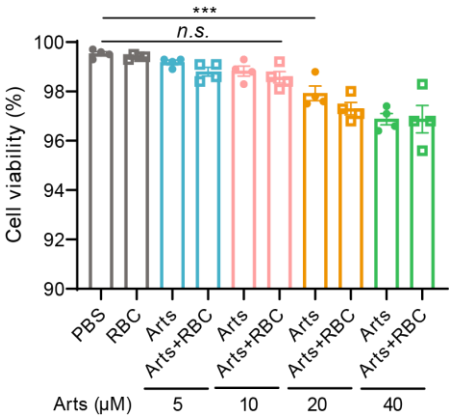


Figure S15. The effect of different concentrations of Arts on the viability of macrophages. A series of dilutions of Arts or Arts combined with RBC were added to the RAW264.7 cells (n = 4). Data are mean ± s.e.m. Statistical analysis was performed using two-sided unpaired Student's *t*-tests. $***P < 0.001$, *n.s.* means no significance.

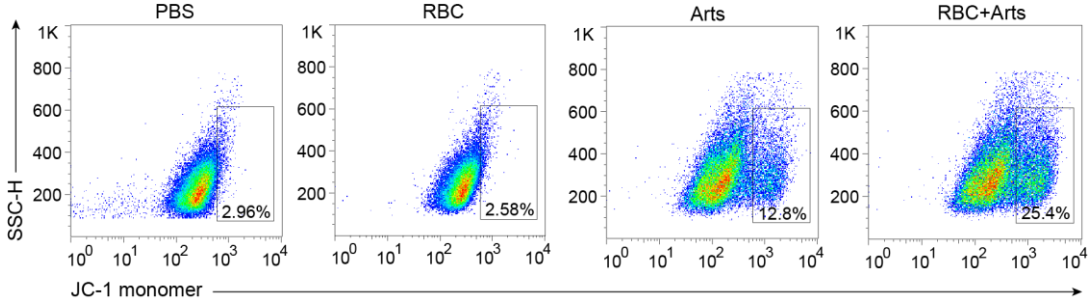


Figure S16. Representative flow cytometry dot plot of JC-1 stained macrophages.

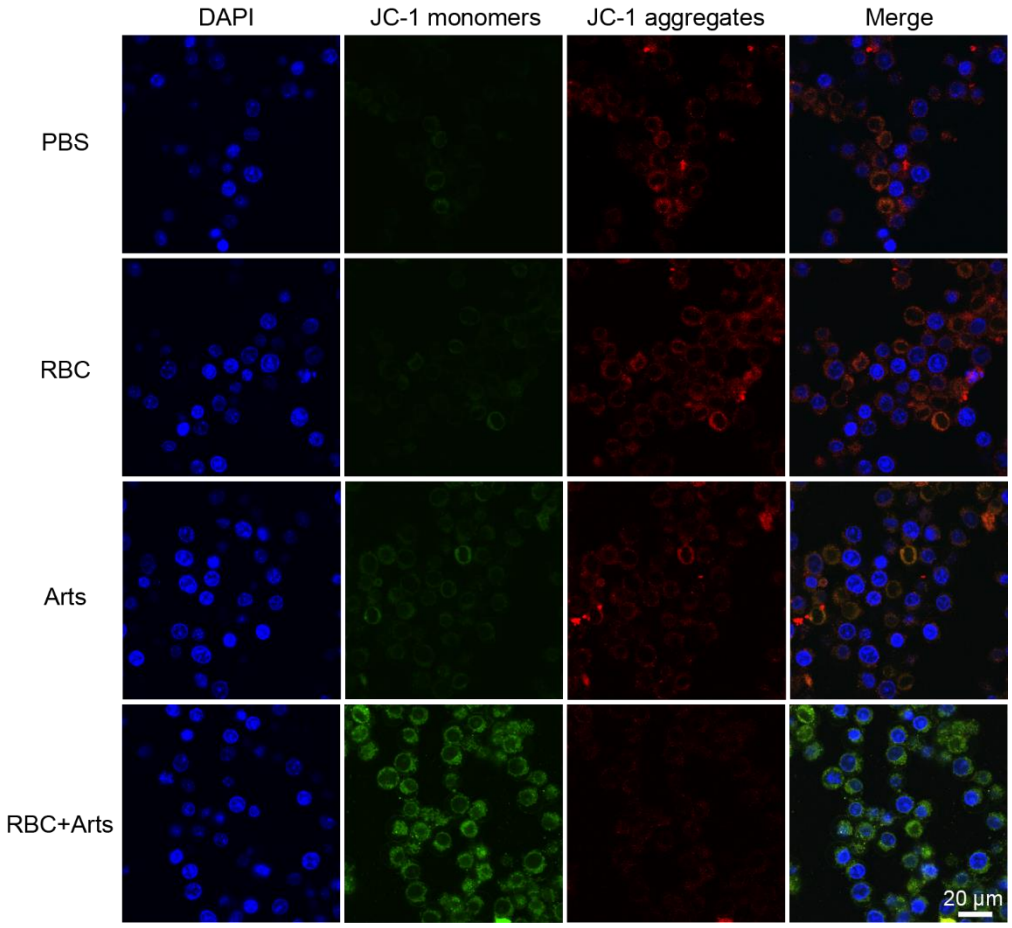


Figure S17. Representative fluorescent images of mitochondrial membrane potential of macrophages treated with RBC and Arts by staining JC-1. Scale bar, 20 μm.

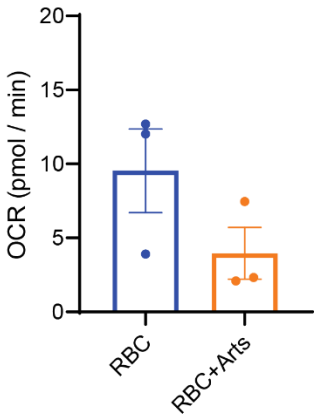


Figure S18. The effects of RBC and Arts on mitochondrial oxidative respiration. The cellular oxygen consumption rate (OCR) of RAW264.7 cells after treatment with RBC and Arts for 12 h (n = 3). Data are mean ± s.e.m.

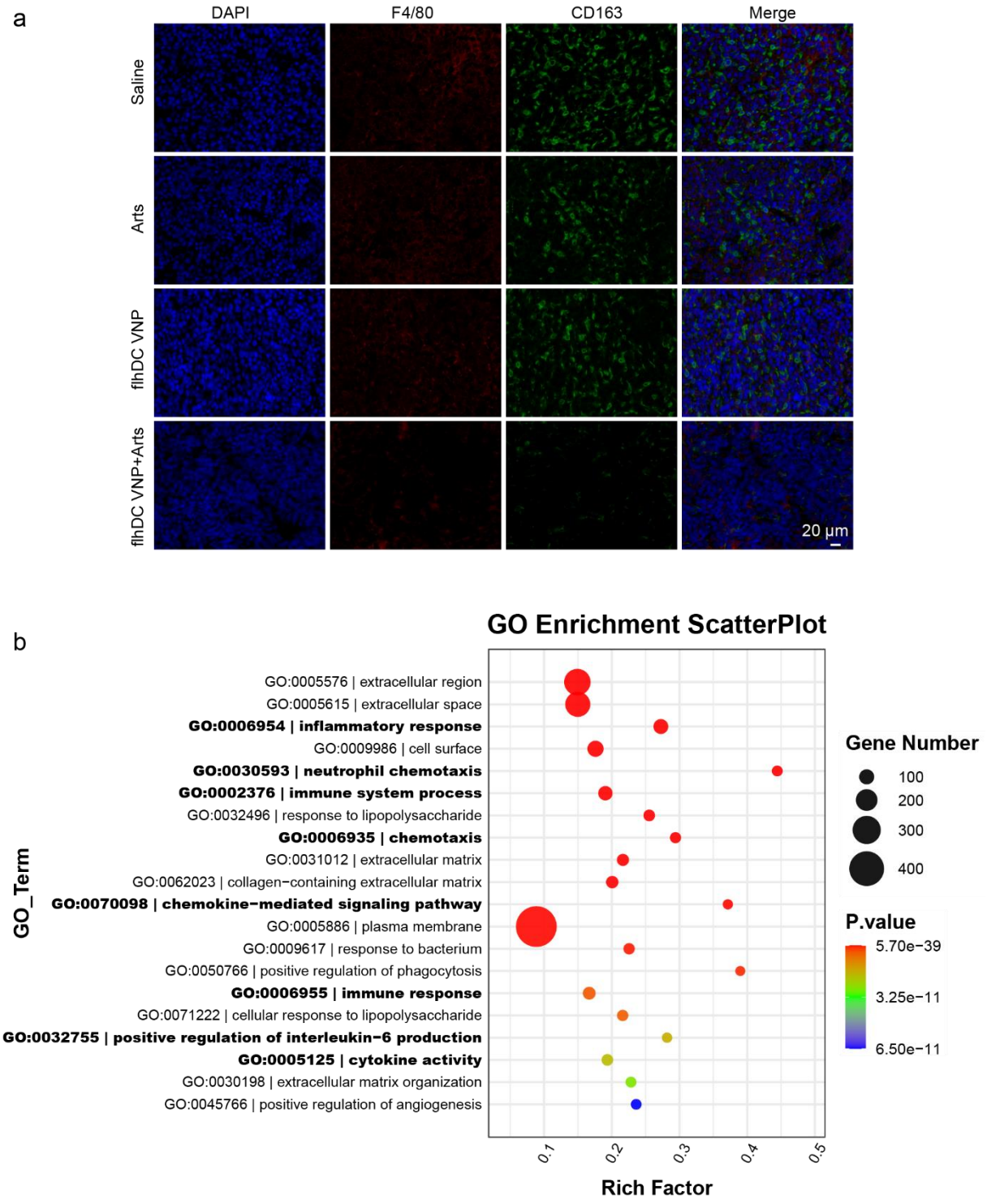


Figure S19. Characterization of tumor immune microenvironment. a) Representative fluorescent images of F4/80^{+}CD163^{+} macrophages in tumor after different treatments. Scale bar, 20 μm. b) GO enrichment regulation in tumor treated with Arts and flhDC VNP + Arts (flhDC VNP + Arts vs Arts).

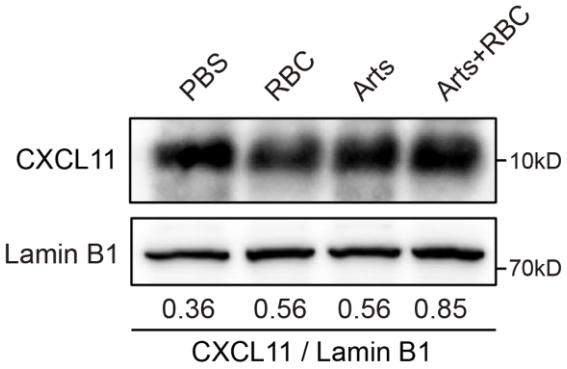


Figure S20. Secretion of chemokines of RAW264.7 cells after different treatments. Western blot analysis of CXCL11 in RAW264.7 cells after different treatments.

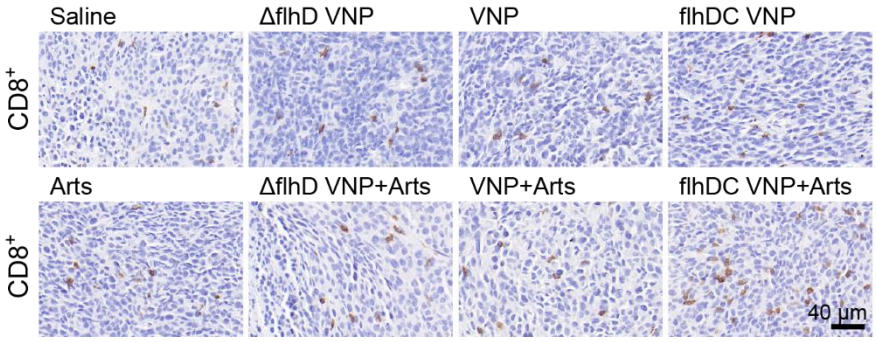


Figure S21. Representative immunohistochemical images of $CD8^+$ T cells in tumor in the xenograft CT26 tumor model. Scale bar, 40 μm.

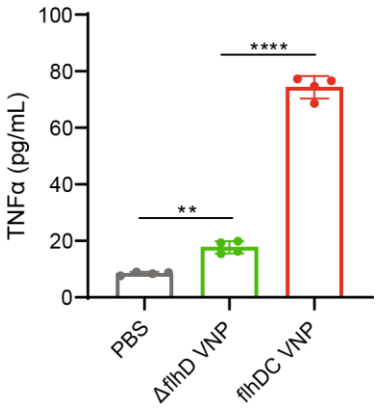


Figure S22. Secretion of TNFα by RAW264.7 cells treated with ΔflhD VNP and flhDC VNP. Data are mean ± s.e.m. Statistical analysis was performed using one-way ANOVA with Dunnett's test. $^{**}P < 0.01$, $^{****}P < 0.0001$.

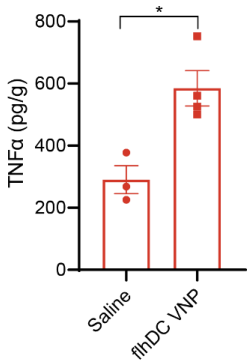


Figure S23. Concentration of TNFα in tumor after treatment with flhDC VNP (saline, n = 3; flhDC VNP, n = 4). Data are mean ± s.e.m. Statistical analysis was performed using two-sided unpaired Student's t-tests. *$P < 0.05$.

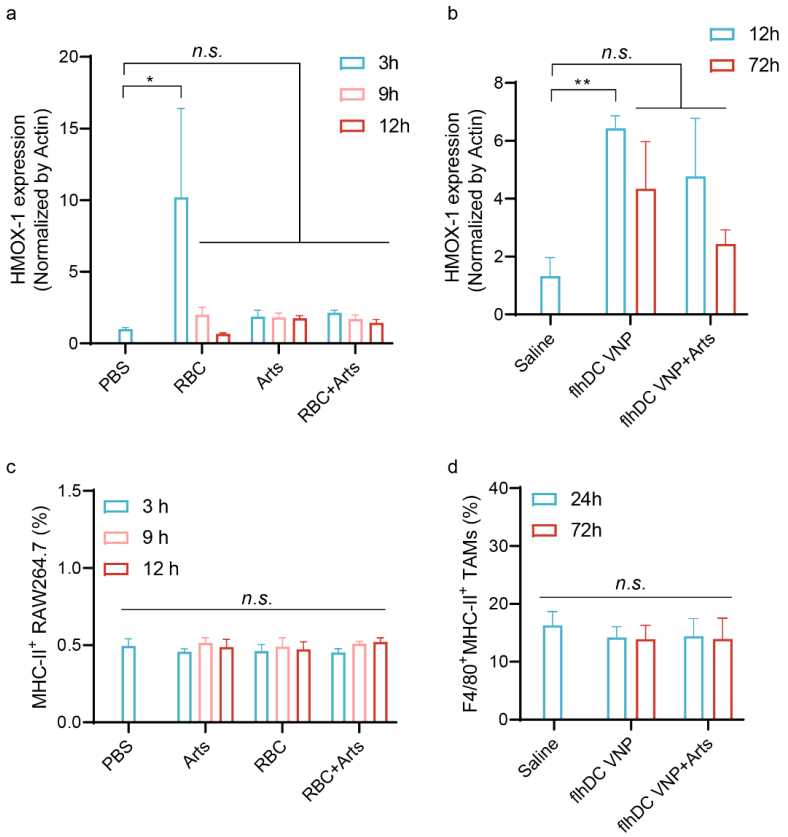


Figure S24. The effects on the expression of HMOX-1 and MHC-II of macrophages after different treatments. a,b) qPCR detected the expression changes of HMOX-1 of RAW264.7 cells (a, n = 8) and tumor (b, n = 3). c,d) Flow cytometric analysis of MHC-II$^+$ RAW264.7 cells (c, n = 4) and F4/80$^+$MHC-II$^+$ TAMs in tumor (d; saline, n = 3; flhDC VNP, flhDC VNP + Arts, n = 4) after different treatments. In (a-d), data are mean ± s.e.m. Statistical analysis was performed using one-way ANOVA with Dunnett's test (a, c, d), two-sided unpaired Student's t-tests (b). *$P < 0.05$, **$P < 0.01$, *n.s.* means no significance.

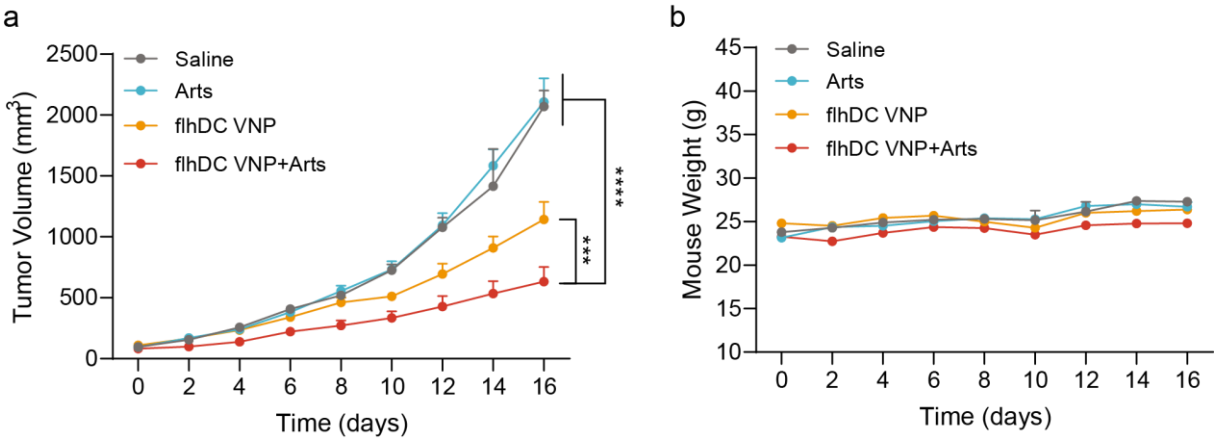


Figure S25. a,b) Average tumor growth curves (a) and mouse weight (b) after different treatments twice in the xenograft colon tumor model (n = 9).In (a, b), data are mean ± s.e.m. Statistical analysis was performed using two-way ANOVA with correction for multiple comparisons (a). ***$P < 0.001$, ****$P < 0.0001$.

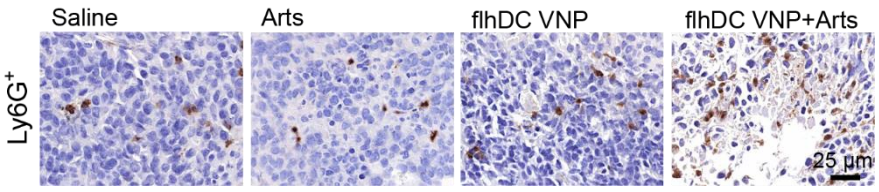


Figure S26. Representative immunohistochemical images of $Ly6G^+$ neutrophils in the orthotopic CT26 tumor model. Scale bar, 25 μm.

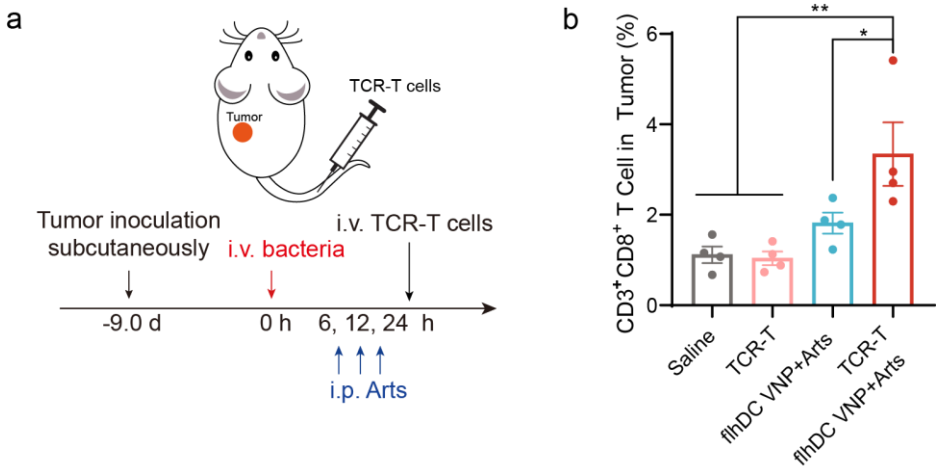


Figure S27. a) Schematic of the treatment schedule in adoptive TCR-T cell therapy.
b) Flow cytometric analysis of $CD3^+CD8^+$ T cells in tumor in adoptive TCR-T cell therapy (n = 4). In (b), data are mean ± s.e.m. Statistical analysis was performed using one-way ANOVA with Dunnett's test (b). *$P < 0.05$, **$P < 0.01$.

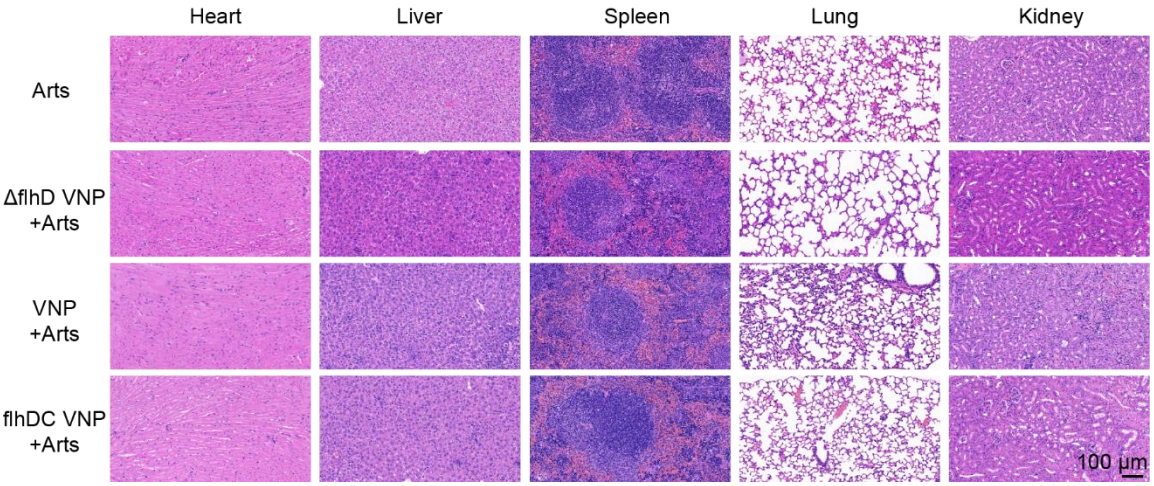


Figure S28. H&E from major organs after systemic administration of bacteria and Arts. The major organs of mice were collected including heart, liver, spleen, lung, and kidney on the 10th day of the antitumor efficacy assay in the xenograft colon tumor model. Scale bar, 100 μm.

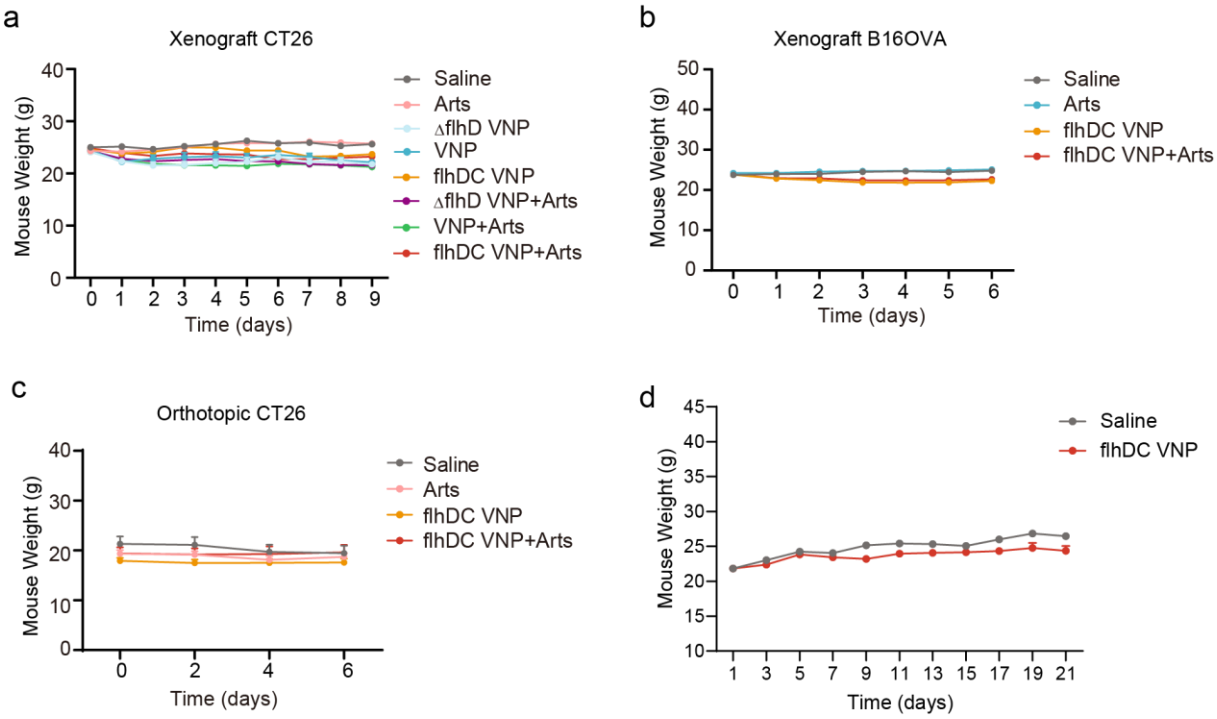


Figure S29. a-c) Mouse weight in xenograft CT26 (a), xenograft B16OVA (b), orthotopic CT26 (c) tumor model. d) Mouse weight after multiple injections of flhDC VNP. In (a-d), data are mean ± s.e.m.